Thin Solid Films 534 (2013) 603–608

Contents lists available at SciVerse ScienceDirect

Thin Solid Films

journal homepage: www.elsevier.com/locate/tsf

Analysis of electrical properties and deep level defects in undoped GaN Schottky barrier diode

Koteswara Rao Peta [a], Byung-Guon Park [a], Sang-Tae Lee [a], Moon-Deock Kim [a,*], Jae-Eung Oh [b], Tae-Geun Kim [c], V. Rajagopal Reddy [d]

[a] Department of Physics, Chungnam National University, 220 Gung-dong, Yuseong-gu, Daejeon 305-764, Republic of Korea
[b] School of Electrical and Computer Engineering, Hanyang University, Ansan 425-791, Republic of Korea
[c] Department of Electronic Engineering, Korea University, Seoul 136-075, Republic of Korea
[d] Department of Physics, Sri Venteswara University, Tirupathi 517-502, India

ARTICLE INFO

Article history:
Received 23 January 2012
Received in revised form 23 January 2013
Accepted 25 January 2013
Available online 4 February 2013

Keywords:
III–V semiconductors
Schottky barrier diodes
Deep level defects
Leakage current

ABSTRACT

Electrical and deep level defects have been investigated in GaN Schottky barrier diode (SBD) in the temperature ranging from 125 K to 425 K. The study was carried out by combined current density–voltage (*J*–*V*), capacitance–voltage (*C*–*V*) and deep level transient spectroscopy (DLTS) characterization techniques. It is found that the ideality factor *n* of the diode decreases and the corresponding Schottky barrier height (SBH) increases with increasing temperature, which indicates the barrier in-homogeneity at metal/semiconductor interface. Thermionic emission with Gaussian distribution of SBHs is thought to be responsible for the electrical behavior of the diode over the temperature region. The possible explanation for this discrepancy in the estimated SBHs from *J*–*V* and *C*–*V* is presented. The DLTS measurement has revealed two deep level traps in GaN with activation energies $E_c - 0.23$ eV and $E_c - 0.45$ eV having different capture cross-sections. In addition, we observed that the reverse leakage current in GaN SBD above 275 K is due to Frenkel–Poole emission (FPE). The estimated emission barrier height by FPE model is about ~0.25 eV. Hence, the reverse leakage current is due to the emission of electrons from the trap state near the metal–semiconductor interface into a continuum of states, associated with conductive dislocations.

1. Introduction

During the last few decades, gallium nitride (GaN) is believed to be a promising material for electronic and photoelectric devices. Since it has wide direct bandgap (3.4 eV at room temperature [1]), high beak-down field (2.3 MV/cm [2]), and high saturation velocity (2.7×10^7 cm/s [3]). This material can also able to support a hetero-structure device technology with high two-dimensional electron gas carrier density and mobility [4]. In particular, GaN is a very promising semiconductor material for realization of high electron mobility transistors [5], metal–semiconductor field-effect transistors [6], light emitting diodes [7] and laser diodes [8]. Undoped GaN usually reveal n-type conductivity in hetero-structure devices, which is responsible for parallel conduction and is critical for making more reliable and high performance oriented devices. More detailed characterization is needed for the complete understanding of relevant mechanisms involved in charge transport, which still remains a challenging problem. For the past few years, extensive work is being carried out on GaN based Schottky barrier diodes (SBDs) [9–14] and a variety of methods were developed to curb the high leakage at reverse bias in GaN SBD [15,16]. One of the active research deals with analysis of electrical and deep level properties of GaN SBD. This gives a better picture of the conduction mechanism, and allows understanding of different aspects involved in the reverse leakage current transport mechanism. Zhang et al. reported that reverse leakage current at high temperatures, is due to Frankel–Poole emission (FPE) in both GaN and AlGaN SBDs [17]. Recently, Rao et al. investigated the reverse leakage current mechanism on Ga-polarity GaN SBD grown by molecular beam epitaxy on Si(111) [18].

In the present work, we have been investigating electrical and deep level defect properties of GaN SBD grown by metal-organic chemical vapor deposition (MOCVD) using current density–voltage (*J*–*V*), capacitance–voltage (*C*–*V*) and deep level transient spectroscopy (DLTS) characterization techniques.

2. Experimental details

The sample used in this study is 3.5 μm GaN film, grown on (0001) surface of the sapphire substrate by MOCVD. A nucleation GaN (30 nm) buffer layer was grown at 550 °C, followed by a 3.5 μm thick unintentionally doped GaN layer deposited at 1130 °C. The estimated room temperature mobility and concentration of electrons in GaN by Hall measurement are 526 $cm^2/V\,s$ and ~5.2×10^{16} cm^{-3}

* Corresponding author. Tel.: +82 42 821 5452; fax+82 42 822 8011.
E-mail address: mdkim@cnu.ac.kr (M.-D. Kim).

0040-6090/$ – see front matter © 2013 Elsevier B.V. All rights reserved.
http://dx.doi.org/10.1016/j.tsf.2013.01.100

respectively. The sheet resistance of GaN is determined to be 802 Ω/. Then, for Schottky diode fabrication, square-shaped Ohmic contact was formed by standard photolithography on GaN surface using a Ti/Al/Ni/Au (30/40/40/200 nm) metal alloy. Ohmic metallization was annealed at 800 °C for 30 s in N_2 ambient in rapid thermal annealing system before Schottky metal deposition. Square Schottky contacts of Ni/Au (30/200 nm) with an area of 390×390 μm^2 were deposited in the center of the Ohmic contact by e-beam evaporation. The temperature dependent current–voltage characteristics of the Schottky diode were performed in vacuum using Keithley measurement unit (Model no. 236) in steps of 50 K from 125 K to 425 K, followed by capacitance–voltage measurement by Boonton capacitance meter (Model no. 7200). LN_2 cooled cryostat is used for temperature dependent measurement. Then, DLTS measurements were performed over a temperature range of 125–425 K. Typically, a quiescent reverse bias voltage of −2.5 V was employed, with filling voltage of 0.5 V.

3. Results and discussion

Fig. 1(a) is the semi logarithmic forward current density–voltage (J–V) characteristics of undoped GaN SBD in the temperature ranging from 125 K to 425 K in steps of 50 K. The diode exhibits two different exponential segments at low and high current levels in bias regions of $0<V<1.2$ and >1.2 V respectively. At low current levels (<1.2 V) as the temperature increases thermionic emission is the dominant conduction mechanism across the metal/semiconductor interface. Since, the barrier heights are lowered due to the increase in electron thermal energy [19]. At higher current level (>1.2 V) a decrease in dark current with increasing temperature is mainly due to the voltage drop across the series resistance (R_s) of SBD. The resistivity of undoped GaN increases with increasing temperature due to the decrease in electron mobility with temperature [9,11]. The increase of GaN resistivity causes an increase of R_s, which leads to downward J–V curve at voltages (>1.2 V). The reverse bias current density increases with increasing temperature attributed to the presence of deep level defects in the near surface region of GaN. The dominant reverse leakage current mechanism through the defect level is given in detail in the last section.

For forward bias, by neglecting the effect of minority carriers on the $V>3kT/q$ and the account of R_s on low current level, thermionic emission (TE) model is valid over GaN SBDs. The J–V relationship by TE model is given by the following relation [20,21]

$$J = J_0 \exp\left(\frac{qV}{nkT}\right)\left[1-\exp\left(\frac{-qV}{kT}\right)\right] \quad (1)$$

where J_0 is the saturation current density and it is defined by $J_0 = A^*T^2\exp\left(\frac{-q\varphi_{b0}}{kT}\right)$, n is the ideality factor, A^* is the effective Richardson's constant (26.4 A cm^{-2} K^{-2} for GaN [9]), φ_{b0} is the zero bias Schottky barrier height (SBH) and can be calculated using the obtained J_0 from the intercept of extrapolation for linear fit of J–V curve to zero voltage using the equation

$$\varphi_{b0} = \frac{kT}{q}\ln\left(\frac{A^*T^2}{J_0}\right). \quad (2)$$

The 'n' presents how closely the diode follows the ideal diode equation and can be determined from the slope of the linear region of the semi-log forward bias J–V characteristics using Eq. (1). The ideality factor 'n' can be written in the form of

$$n = \frac{q}{kT}\left(\frac{dV}{d(\ln J)}\right). \quad (3)$$

Fig. 2 is the graphical representation of the estimated experimental φ_{b0} and n versus temperature. The experimental values of φ_{b0} and n ranged from 0.42 eV and 4.3 (at 125 K) to 1.07 eV and 1.1 (at 425 K), respectively. The experimental values of n monotonously increase with decreasing temperature (Fig. 2) is attributed to the current transport across the metal/semiconductor interface is a temperature activated process; electrons at low temperatures are able to surmount the lower barriers [10,22,23]. Therefore, the current transport will be dominated by the current flowing through the patches of lower SBHs [22,24,25]. As shown in Fig. 2, the values of φ_{b0} of the GaN Schottky diode calculated from J–V characteristics show an unusual behavior with the increase of temperature. Such temperature dependence of SBH is attributed to the barrier in-homogeneity at metal/semiconductor interface.

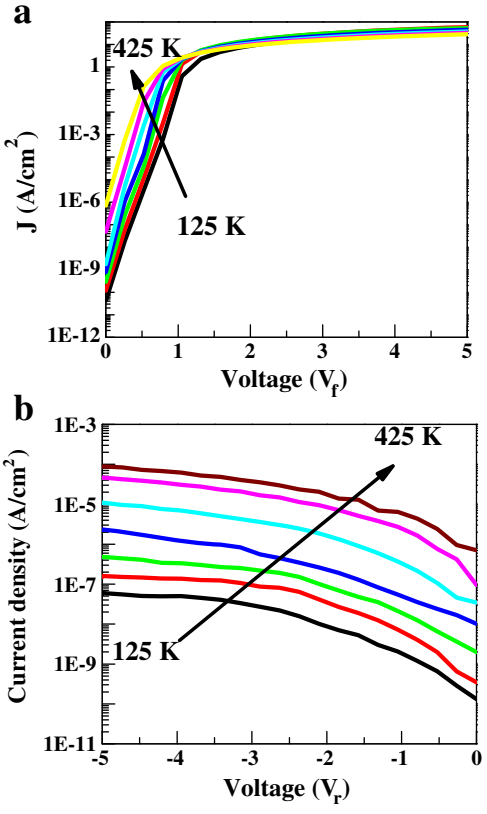

Fig. 1. (a) The experimental semi-logarithmic forward current density–voltage (J–V) characteristics of GaN SBD in the temperature ranging from 125 to 425 K in steps of 50 K. (b) Reverse bias current density versus voltage characteristics for GaN SBD in wide temperature range.

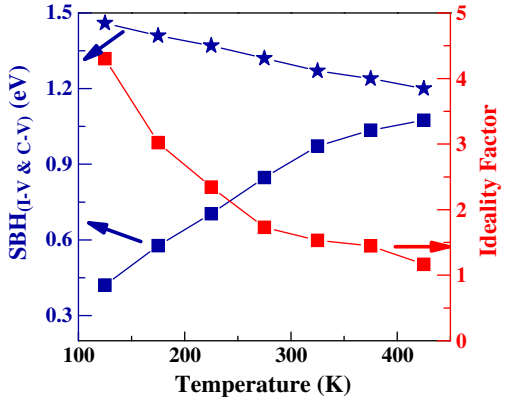

Fig. 2. The temperature dependent SBHs estimated from J–V (squares) and C–V (stars) characteristics and ideality factor for GaN SBD.

In order to explain such behavior of φ_{b0} and n, TE mechanism with a Gaussian distribution (GD) of the SBHs has been suggested [11,26,27]. Hence, the SBHs with mean value $\overline{\Phi}$ and standard deviation σ_0 is given as

$$\varphi_{b0} = \overline{\Phi}(T=0) - \frac{q\sigma_0^{\,2}}{2kT}. \tag{4}$$

The temperature dependency of σ_0 is usually small and can be neglected [28]. In addition, the observed variation of the ideality factor n with temperature T in the model is given by [29]

$$\left(\frac{1}{n}-1\right) = \rho_2 - \frac{q\rho_3}{2kT} \tag{5}$$

where ρ_2 and ρ_3 are voltage coefficients which may depend on temperature, and they quantify the voltage deformation of the SBH distribution. Since the mean barrier height ($\overline{\Phi}$) and σ_0 are linearly bias dependent of GD parameters, such that SBH $=\overline{\Phi}+\rho_2 V$ and standard deviation $\sigma_s = \rho_{so}+\rho_3 V$. Thus the plot of SBH versus $(2kT)-1$ (Fig. 3(a)) should be a straight line which gives $\overline{\Phi}$ and σ_0 from the intercept and slope respectively. The values of $\overline{\Phi}$ and σ_s were found to be 1.31 eV and 143 meV respectively. Which are in good agreement with the reported $\overline{\Phi}$ and σ_s values [11,30]. The best rectifier with barrier homogeneity has lower value of standard deviation. But, the obtained value of σ_s is not small when compared with $\overline{\Phi}$ value and it indicates barrier in-homogeneity at metal–semiconductor interface [10]. The values of ρ_2 and ρ_3 were determined from the intercept and slope of the plot $(1/n-1)$ versus $(2kT)-1$ (Fig. 3(a)). The estimated values of ρ_2 and ρ_3 are 17 and 22 meV respectively. Hence, the existence of high ideality factor at low temperature is due to the in-homogeneity and potential fluctuations in the barrier. Fig. 3(b) is the plot between $\ln(J_0/T^2)-(e^2\sigma_0^{\,2}/2k^2T^2)$ versus $1/T$ is called the modified Richardson's plot. The estimated φ_{b0} ($T=0$ K) and Richardson's constant (A^*) from slope and intercept of linear fit are 1.29 eV and 26.05 A cm^{-2} K^{-2} respectively. It is observed that, obtained SBH and A^* from modified Richardson's plot is in good agreement with the value of mean SBH ($\overline{\Phi}$) (1.31 eV) estimated from φ_{b0} versus $1/2kT$ (Fig. 3(a)) and the known theoretical value 26.4 A cm^{-2} K^{-2} of GaN respectively. Hence, the barrier in-homogeneities at metal/semiconductor interface for GaN SBD is successfully explained by TE with GD of barrier over the SBHs.

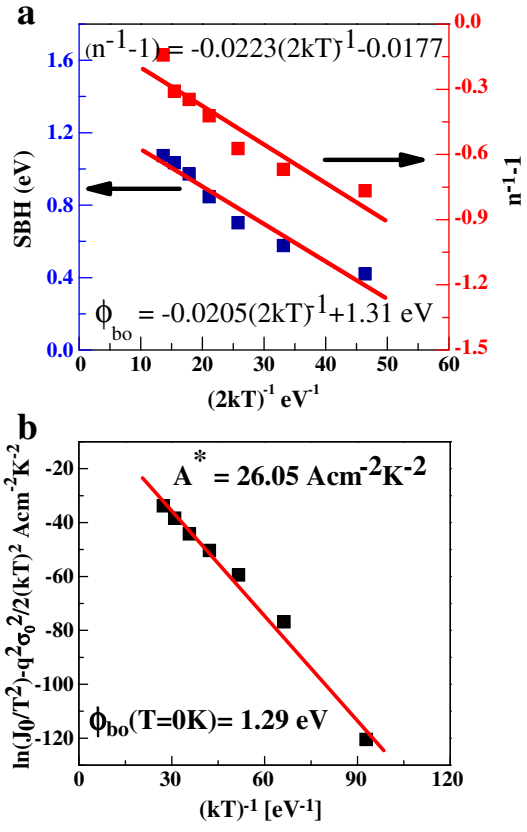

Fig. 3. (a) SBH and $(n^{-1}-1)$ versus $(2kT)^{-1}$ plots for GaN SBD using Gaussian distribution over the SBHs, (b) Modified Richardson's plot of $\ln(J_0/T^2)-(q^2\sigma_0^2/2k^2T^2)$ versus $(kT)^{-1}$.

The capacitance–voltage (C–V) measurements were performed at sufficiently high frequency of 1 MHz, because the interface state charges at this high frequency, do not contribute to the capacitance of the diode. This will occur when the time constant is too long to permit the charge to move in and out of the interface states in response to an applied signal [31,32]. The dark C–V characteristics have been analyzed using the depletion capacitance equation of unit area of n-type SBDs by the following equation [33]

$$\frac{C}{A} = \sqrt{\frac{q\varepsilon_s(N_D-N_A)}{2(V_{bi}+V-kT/q)}} \tag{6}$$

where C is the capacitance, A is the area, ε_s is the dielectric constant (for GaN $\varepsilon_s = 9\varepsilon_0$ [11]), V is the applied voltage, V_{bi} is the built-in potential, and N_D-N_A is the net donor concentration. The built-in potential is related to the SBH by the relation

$$\varphi_{C-V} = V_{bi} + V_0. \tag{7}$$

Here $V_0 = (kT/q)\ln(N_C/N_D)$, where N_C is the effective density of states in the conduction band ($N_C = 2.3\times10^{18}$ cm^{-3} for GaN at room temperature). The C–V results for the SD plotted as C^{-2} versus V gives a straight line, whose slope of linear fit is equal to $2/[q\varepsilon_s(N_D-N_A)]$, and with an intercept $-V_{bi}+kT/q$ on X-axis.

Fig. 4(a) shows the C^{-2} versus V characteristics of SBD in the temperature ranging from 125 K to 425 K in steps of 50 K. The plots are linear in the whole temperature range. This indicates a constant net donor concentration in the depletion region in the absence of metal/semiconductor interaction. The carrier density of an undoped GaN SBD is ~7.0×10^{16} cm^{-3} at room temperature. The extracted built-in potential fairly increases with decreasing temperature and can be seen in Fig. 4(b). The net donor concentration decreases with the decrease in temperature (Fig. 4(b)) which may be accompanied with depletion layer width and is attributed to the measured capacitance influenced by carrier trapping levels in the semiconductor. The SBH values extracted from the C–V increase with decreasing temperature and are in opposite manner to SBH from J–V Characteristics (Fig. 2). This discrepancy is due to the existence of excess capacitance at the interfacial layer due to deep level traps in the semiconductor and the barrier in-homogeneity at metal/semiconductor interface.

DLTS measurements were carried at quiescent reverse bias of −2.5 V, a filling pulse of 0.5 V with pulse duration of $t_p = 28$ ms was used to ensure complete filling of the trap in the temperature ranging from 125 K to 425 K. The transient capacitance signal, acquired by using a test ac signal of 1 MHz with an emission rate window $e_n = 200$ s^{-1} was recorded. Fig. 5(a) shows DLTS spectrum for undoped GaN SBD. Two well resolved electron traps E_1 and E_2 were observed, which are peaked at 185 K and 335 K. The activation energy and capture cross section of deep level defect can be obtained from the slope and intercept of linear fit to Arrhenius plot, which was plotted using the emission rate and peaked temperature of DLTS spectra of different rate windows. According to the principle of detailed balance,

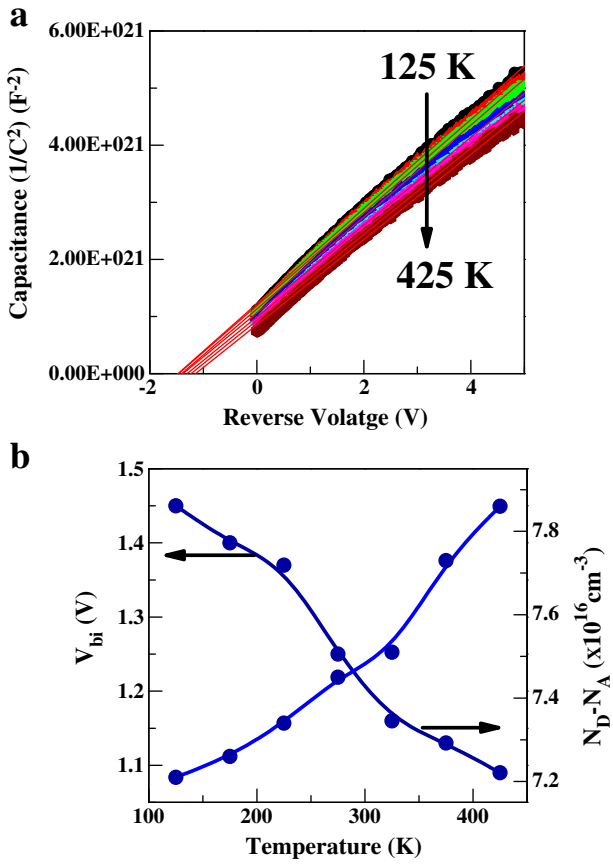

Fig. 4. (a) Characteristic plot for C^{-2} versus V for GaN SBD in the temperature ranging from 125 to 425 K in steps of 50 K. (b) The variation of built-in potential and net donor density as a function of temperature for GaN SBD.

the electron emission rate (e_n) related with trap parameters is given by [33]

$$e_n = \sigma_n K T^2 \exp\left(\frac{-E_T}{kT}\right) \tag{8}$$

where σ_n is the electron capture cross-section, K is a constant, T is the absolute temperature and k is the Boltzmann constant. Then for experimental exponential transients we have

$$\tau_{\max} = \frac{t_2 - t_1}{\ln\left(\frac{t_2}{t_1}\right)} = {e_n}^{-1}. \tag{9}$$

Hence, activation energy and capture cross section of these traps are determined by Arrhenius analysis $\ln(e_n/T^2) = \ln(K\sigma_n) - (E_a/kT)$ using DLTS spectra for different emission rate windows and can be seen in Fig. 5(a). Fig. 5(b) shows the Arrhenius plot $\ln(e_n/T^2)$ versus $1000/T$ for E_1 and E_2. The estimated activation energies and capture cross sections are $E_c - 0.23$ eV, $\sim 6.17\times10^{-16}$ cm^2 for E_1 and, $E_c - 0.45$ eV, $\sim 6.17\times10^{-14}$ cm^2 for E_2 respectively. The calculated trap density is about $\sim 3.2\times10^{13}$ cm^{-3} for E_1 and, $\sim 2.7\times10^{15}$ cm^{-3} for E_2 respectively. The intensity of the peaks is attributed to the concentration of the trap levels. We interpret that E_1 and E_2 correspond to the deep level defects with energies 0.18 eV and 0.49 eV [34]. The physical source of E_1 level may be associated with nitrogen vacancies and have often been observed in the GaN film grown by different methods [34–36]. The E_2 level is a commonly identified defect level in GaN, and is comparable with the trap level $E_c - 0.60$ eV in Ga-face GaN grown by molecular beam epitaxy, reported by Arehart et al. [35]. But still the source of this defect is unclear. A. R. Arehart et al.

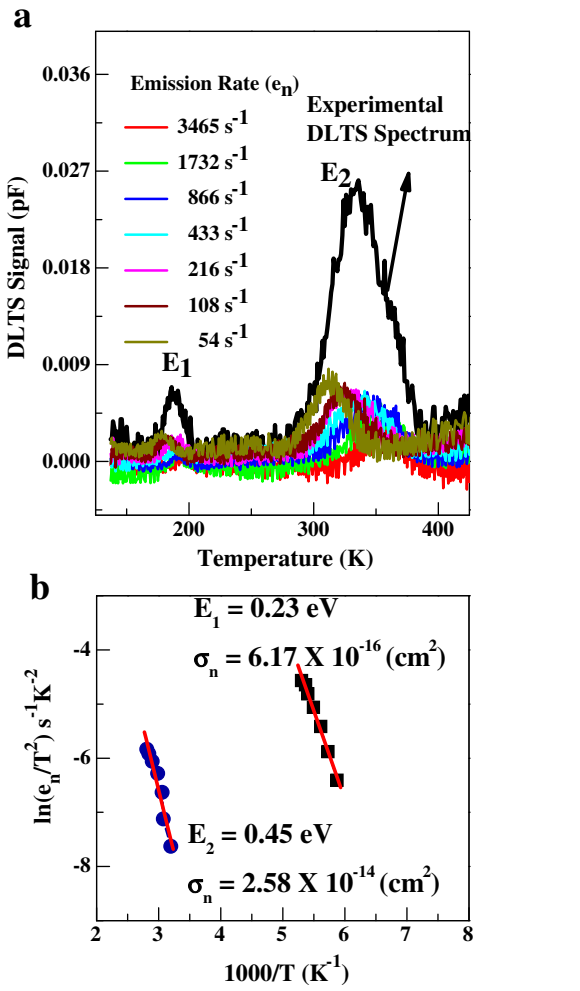

Fig. 5. (a) DLTS spectrum of GaN SBD measured in the temperature range 125 K–425 K ($V_r = -2.5$ V, $V_f = 0.5$ V, $e_n = 200$ s^{-1}, and $t_P = 28$ ms) and DLTS spectra for seven different emission rate windows determined by the values of t_1 and t_2 for GaN Schottky diode. (b) The Arrhenius plot of $\ln(e_n/T^2)$ versus $1000/T$.

[37] explained the nature of E_2 defect by capture kinetics. The concentration correlation ascribed to a point defect dislocation complex is associated with threading dislocation density [37].

Fig. 1(b) shows the reverse bias J–V characteristics as a function of measured temperature, the leakage current increases with temperature. The estimated SBH at 275 K by standard thermionic emission is 0.80 eV. According to Chikhaoui et al. [38], when the SBH increases with temperature, the leakage current by thermionic emission and tunneling over the Schottky barrier are negligible. Therefore, we assume FPE at the metal–semiconductor interface. In this model the current flow due to the electric field enhanced thermal emission from the trap state into a continuum of electronic states and the associated current density is given by [18,38]

$$J_r = CE_r \exp\left[-\frac{q\left(\varphi_t - \sqrt{qE_r/\pi\varepsilon_0\varepsilon_s}\right)}{kT}\right]. \tag{10}$$

Hence, the current transport by FPE, that is $\ln(J/E_r)$ should be a linear function of $\sqrt{E_r}$

$$\ln(J/E_r) = \frac{q}{kT}\sqrt{\frac{qE_r}{\pi\varepsilon_0\varepsilon_s}} - \frac{q\varphi_t}{kT} + \ln C = B(T)\sqrt{E_r} + A(T). \tag{10a}$$

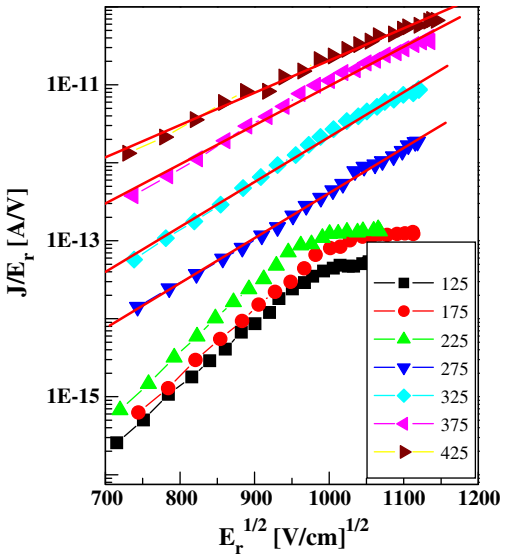

Fig. 6. The characteristic plot of $\ln(J/E_r)$ versus $E_r^{1/2}$ for undoped GaN SBD.

Here $A(T)$ and $B(T)$ are the intercept and slope of the $\ln(J/E_r)$ versus $E_r^{1/2}$ plot and are defined as

$$A(T) = -\frac{q\varphi_t}{kT} + \ln C \tag{10b}$$

$$B(T) = \frac{q}{kT}\sqrt{\frac{qE_r}{\pi\varepsilon_0\varepsilon_s}} \tag{10c}$$

where J is the current density and E_r is the electric field at the semiconductor surface. We observed a linear dependence of $\ln(J/E_r)$ on $E_r^{1/2}$ above 275 K (Fig. 6(a)) indicates that, the electric field enhanced by thermal emission from a trapped state into a continuum of electronic states at metal/semiconductor interface [17], in which usually, but not necessarily, the conduction band in an insulator. Fig. 7(a) and (b) shows the plots of $A(T)$ and $B(T)$ versus $1/T$. Here $A(T)$ and $B(T)$ values are obtained by intercepts and slopes of linear fits to the characteristic curves of $\ln(J/E_r)$ versus E_r plot. The estimated dielectric constant and emission barrier height from the slopes of $A(T)$ and $B(T)$ versus $1/T$ are $\varepsilon_s = 10.3$ and the emission barrier height $(\phi_t) = 0.25$ eV respectively and these values are in good agreement with the values obtained by Zhang et al. [17]. Thus, the process governs that the leakage current is due to FPE from trapped state within the semiconductor. And most likely a trap state near the metal/semiconductor interface into a continuum of states associated with a conductive dislocation. The carrier transport from the metal contact into the conductive dislocation must occur via a trap state rather than by direct thermionic emission from the metal from above 275 K for GaN SBD.

4. Conclusion

The electrical properties and deep level defects of undoped GaN SBD have been reported by J–V, C–V and DLTS techniques in the temperature ranging from 125 to 425 K in steps of 50 K. The experimental values of φ_{b0} and n ranged from 0.42 eV and 4.3 (at 125 K) to 1.07 eV and 1.1 (at 425 K), respectively for GaN SBD. The donor concentration and built-in potentials were calculated using the C–V temperature characteristics measured at 1 MHz frequency. The discrepancy between the SBHs obtained from J–V and C–V measurements are explained by introducing a spatial distribution of SBHs due to barrier height in-homogeneities, which occur at the metal/semiconductor junction interface. The DLTS revealed two dominant deep level defects with activation energies

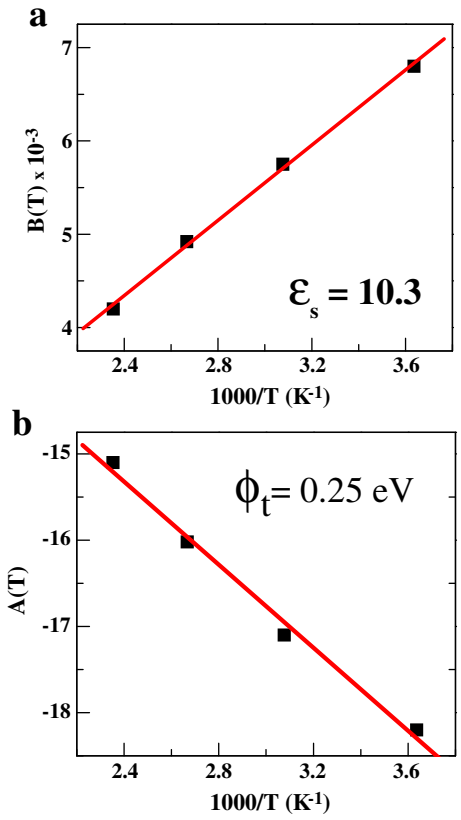

Fig. 7. (a) The plot of $B(T)$ versus $1/T$ for GaN SBD. (b) The plot of $B(T)$ versus $1/T$ for GaN SBD. Here $B(T)$ and $A(T)$ are slope and intercept of a linear fit for $\ln(J/E_r)$ versus $E_r^{1/2}$ plot (Fig. 6) as a function of temperature respectively.

$E_c - 0.23$ eV and $E_c - 0.45$ eV located at 185 K and 335 K in GaN with different capture cross sections measured at emission rate window $e_n = 200\ s^{-1}$. The reverse leakage current mechanism is analyzed by Frankel–Poole emission effect. The estimated emission barrier height by FPE is 0.25 eV. It is suggested that, the leakage current is due to the field enhanced emission of electrons from the trapped state associated with conductive dislocations from above 275 K.

Acknowledgments

This research was supported by Basic Science Research Program, Leading Foreign Research Institute Recruitment Program through the National Research Foundation of Korea (NRF) funded by the Ministry of Education, Science and Technology (2011-0026194/2012-00109) and by the National Research Foundation of Korea (NRF) grant funded by the Korea government (MEST) (2011-0016618).

References

[1] B. Monemar, Phys. Rev. B 10 (1974) 676.
[2] I.B. Rowena, S.L. Selvaraj, T. Egawa, IEEE Electron. Device Lett. 32 (2011) 1534.
[3] B. Gelmont, K. Kim, M. Shur, J. Appl. Phys. 74 (1993) 1818.
[4] J. Xue, J. Zhang, W. Zhang, L. Li, F. Meng, M. Lu, J. Ning, Y. Hao, J. Cryst. Growth 343 (2012) 110.
[5] K.H. Lee, P.C. Chang, S.J. Chang, Y.K. Su, C.L. Yu, Appl. Phys. Lett. 96 (2010) 212105.
[6] J.H. Leach, M. Wu, X. Ni, X. Li, U. Ozgur, H. Moekoc, Phys. Status Solidi A 207 (2010) 211.
[7] Y.J. Hong, C.H. Lee, A. Yoon, M. Kim, H.K. Seong, H.J. Chung, C. Sone, Y.J. Park, G.C. Yi, Adv. Mater. 23 (2011) 3284.
[8] W.G. Scheibenzuber, U.T. Schwarz, Appl. Phys. Lett. 98 (2011) 181110.
[9] S. Huang, B. Shen, M.J. Wang, F.J. Xu, Y. Wang, H.Y. Yang, F. Lin, L. Lu, Z.P. Chen, Z.X. Qin, Z.J. Yang, G.Y. Zhang, Appl. Phys. Lett. 91 (2007) 072109.
[10] Z. Tekeli, S. Altındal, M. Cakmak, S. Ozcelik, D. Calıskan, E. Ozbay, J. Appl. Phys. 102 (2007) 054510.
[11] Y. Zhou, D. Wang, C. Ahyi, C.C. Tin, J. Williams, M. Park, N.Mark Williams, A. Hanser, Edward A. Preble, J. Appl. Phys. 101 (2007) 024506.

[12] N. Yildirim, K. Ejderha, A. Turut, J. Appl. Phys. 108 (2010) 114506.
[13] T. Sawada, Y. Izumi, N. Kimura, K. Suzuki, K. Imai, S.-W. Kim, T. Suzuki, Appl. Surf. Sci. 216 (2003) 192.
[14] S.H. Phark, H. Kim, K.M. Song, P.G. Kang, H.S. Shin, D.W. Kim, J. Phys. D: Appl. Phys. 43 (2010) 165102.
[15] J. Spradlin, S. Dogan, M. Mikkelson, D. Huang, L. He, D. Johnstone, H. Morkoc, R.J. Molnar, Appl. Phys. Lett. 82 (2003) 3556.
[16] E.J. Miller, D.M. Schaadt, E.T. Yu, P. Waltereit, C. Poblenz, J.S. Speck, Appl. Phys. Lett. 82 (2003) 1293.
[17] H. Zhang, E.J. Miller, E.T. Yu, J. Appl. Phys. 99 (2006) 023703.
[18] P.K. Rao, B.G. Park, S.T. Lee, Y.K. Noh, M.D. Kim, J.E. Oh, J. Appl. Phys. 110 (2011) 013716.
[19] A.R. Hefner, R. Singh, J. Lai, D.W. Berning, S. Bouche, C. Chapuy, IEEE Trans. Power Electron. 16 (2001) 273.
[20] S.M. Sze, Physics of Semiconductor Devices, 2nd Edition, John Wiley & Sons, New York, 1981, p. 279, (245).
[21] E.H. Rhoderick, Oxford University Press, Oxford, 1978, p. 121, (136).
[22] S. Chand, J. Kumar, Appl. Phys. A: Mater. Sci. Process. 65 (1997) 497.
[23] S. Zhu, R.L. Van Meirhaeghe, C. Detavernier, G.P. Ru, B.Z. Li, F. Cardon, Solid State Commun. 112 (1999) 611.
[24] A. Tataroglu, S. Altindal, M.M. Bulbul, Microelectron. Eng. 81 (2005) 140.
[25] H. Norde, J. Appl. Phys. 50 (1979) 5052.
[26] S. Zeyrek, S. Altındal, H. Yuzer, M.M. Bulbul, Appl. Surf. Sci. 252 (2006) 2999.
[27] S. Zhu, R.L. Van Meirhaeghe, C. Detavernier, F. Cardon, G.P. Ru, X.P. Qu, B.Z. Li, Solid-State Electron. 44 (2000) 663.
[28] S. Chand, J. Kumar, Semisond. Sci. Technol. 11 (1996) 1203.
[29] J.H. Werner, H.H. Guttler, J. Appl. Phys. 69 (1991) 1522.
[30] Z.Q. Fang, D.C. Look, P. Visconti, D.F. Wang, C.Z. Lu, S.S. Park, Appl. Phys. Lett. 78 (2001) 2178.
[31] S.H. Huang, Y. Tian, F. Lu, Appl. Surf. Sci. 234 (2004) 362.
[32] J.H. Evans-Freeman, M.M. El-Nahass, A.A.M. Farag, A. Elhaji, Microelectron. Eng. 88 (2011) 3353.
[33] D.K. Schroder, Semiconductor Material and Device Characterization, John Wiley & Sons, New York, 1998, p. 173.
[34] W. Gotz, N.M. Johnson, Appl. Phys. Lett. 65 (1994) 463.
[35] A.R. Arehart, T. Homan, M.H. Wong, C. Poblenz, J.S. Speck, S.A. Ringel, Appl. Phys. Lett. 96 (2010) 242112.
[36] P. Hacke, T. Detchprohm, K. Hiramatsu, N. Sawaki, J. Appl. Phys. 76 (1994) 304.
[37] A.R. Arehart, A. Corrion, C. Poblenz, J.S. Speck, U.K. Mishra, S.A. Ringel, Appl. Phys. Lett. 93 (2008) 112101.
[38] W. Chikhaoui, J.M. Bluet, M.A. Poisson, N. Sarazin, C. Dua, C. Bru-Chevallier, Appl. Phys. Lett. 96 (2010) 072107.